Article

Chinese Science Bulletin

SPECIAL ISSUE: Extreme Climate in China

April 2013 Vol.58 No.12: 1436–1442
doi: 10.1007/s11434-012-5540-1

Projected change in the relationship between East Asian summer rainfall and upper-tropospheric westerly jet

DAI Yi[1,2] & LU RiYu[1*]

[1] *National Key Laboratory of Numerical Modeling for Atmospheric Sciences and Geophysical Fluid Dynamics (LASG), Institute of Atmospheric Physics, Chinese Academy of Sciences, Beijing 100029, China;*
[2] *Graduate University of Chinese Academy of Sciences, Beijing 100049, China*

Received August 20, 2012; accepted September 20, 2012; published online November 23, 2012

The authors analyzed the interannual variability in summer precipitation and the East Asian upper-tropospheric jet (EAJ) over East Asia under the Historical and Representative Concentration Pathways Scenarios (RCPs, including RCP4.5 and RCP8.5), using outputs of 17 Coupled Model Intercomparison Project phase 5 (CMIP5) coupled models. The analyzed results indicate that the models can reasonably reproduce relatively stronger interannual variability in both East Asian summer rainfall (EASR) and EAJ. These models can also capture the relationship between the rainfall anomaly along the East Asian rain belt and meridional displacement of the EAJ. Projected results suggest that the interannual variabilities in precipitation along the East Asian rain belt and in the EAJ are enhanced under the scenarios RCP4.5 and RCP8.5 in the 21st century, which is consistent with the previous studies. Furthermore, it is found that the relationship between the East Asian rainfall and the meridional displacement of the EAJ is projected to be stronger in the 21st century under the global warming scenarios, although there are appreciable discrepancies among the models.

East Asian rainfall, East Asian upper-tropospheric jet, interannual variability, relationship, projected change

Citation: Dai Y, Lu R Y. Projected change in the relationship between East Asian summer rainfall and upper-tropospheric westerly jet. Chin Sci Bull, 2013, 58: 1436–1442, doi: 10.1007/s11434-012-5540-1

East Asian summer monsoon has an important social and economic impact in eastern China, the Korean Peninsula and the southern and central Japan. Its variability causes serious floods and droughts, which are the most natural disasters in East Asia, and brings about great damages in this region. The interannual variability in East Asian summer rainfall (EASR) is closely related to the frequency of floods and droughts. Therefore, the interannual variability in rainfall can be approximately used as an important index to measure the possible changes in the frequency of floods and droughts under global warming scenarios.

Many projected results suggested that East Asian summer precipitation will increase in the context of global warming [1–5]. Some other studies indicated that the interannual variability in EASR will be enhanced in the future [6,7], corresponding to the increase of precipitation. On the other hand, Lu and Fu [7] showed that the interanuual variability in EASR is intensified much more remarkably in comparison with summer precipitation itself in East Asia under the global warming scenarios, implying more frequent occurrence of droughts and floods in the future.

The EASR is closely related to the East Asian upper-tropospheric westerly jet (EAJ). As an important component of the atmospheric circulations at the upper troposphere and low stratosphere in the mid latitudes, the EAJ exhibits a unique feature [8,9], and variations in both the location and intensity of the EAJ play a crucial role in influencing weather and climate in East Asia [10–12]. On the interannual timescale, the meridional displacement of the EAJ is the most prominent feature in summer [13] and it is intimately related to the EASR. A southward (northward) displaced EAJ is associated with increased (decreased) EASR

*Corresponding author (email: lr@mail.iap.ac.cn)

in summer [11,14]. Therefore, a better understanding of interannual variability of the EAJ and its relationship with the EASR is crucial for forecasting the occurrence of droughts and floods in East Asia.

There are few studies on the possible change of relationship between EAJ and EASR under the scenario of global warming, despite a lot of research on the projected changes in EASR and some research on the projected change of EAJ [15]. Understanding the change of the relationship, however, enable us not only to study the change of precipitation and EAJ, but also to understand the predictability of East Asian climate.

The results of Lu and Fu [7], who analyzed the CMIP3 outputs, showed that relationship between EAJ and EASRI is not significantly changed in the context of global warming. This insignificance in change of the relationship is manifested by the following two aspects. First, the result of multi-model ensemble (MME) mean shows that the correlation coefficient between the EAJ and EASR do not change obviously. Second, there are great discrepancies in the change of relationship among the individual models, which leads to greater uncertainty in the projected change in the relationship between the EAJ and EASR. The Coupled Model Inter-comparison Project 5 phase (CMIP5) provides another opportunity to estimate the changes of the relationship between the EAJ and EASR, and this is the main motivation of the present study.

1 Data and methods

The results of 17 models in the Coupled Model Inter-comparison Project phase 5 (CMIP5) archive were analyzed. Table 1 lists the basic features of these models. More information can be found at http://www.pcmdi.llnl.gov/cmip5. The number of these models is adequate to estimate qualitatively the uncertainty through analyzing the inter-model discrepancies. Three experiments were used to investigate the projected changes: Historical and two Representative Concentration Pathways Scenarios (RCPs)—RCP4.5 and RCP8.5. The experiment "Historical" represents the simulations of the twentieth century climate, in which the forcing include greenhouse gases, solar forcing, volcanic influences, ozone, and aerosols. The experiments "RCP4.5" and "RCP8.5" are the scenarios that radiative forcing stabilizes at 4.5 W/m^2 and 8.5 W/m^2 by 2100, representing medium stabilization scenario and high emission scenario, respectively.

One of the major differences between the CMIP5 and CMIP3 is that the resolution of the former is generally higher than the latter. As many studies showed, the improvement of the horizontal resolution of climate models is necessary to improve the simulation of East Asian climate [16–18]. The improvement of the resolution and other improvements in CMIP5 models may cause appreciably different results in comparison with CMIP3 models.

Table 1 List of the CMIP5 models analyzed in this study

Model	Country	Atmospheric resolution
CanESM2	Canada	2.8°×2.8°
CCSM4	U.S.A	0.9°×1.3°
CNRM-CM5	France	1.4°×1.4°
Fgoals-g2	China	3.0°×2.8°
Fgoals-s2	China	1.7°×2.8°
GFDL-CM3	U.S.A	2.0°×2.5°
GFDL-ESM2G	U.S.A	2.0°×2.5°
GISS-E2-R	U.S.A	2.0°×2.5°
HadGEM2-CC	Britain	1.3°×1.9°
HadGEM2-ES	Britain	1.3°×1.9°
INMCM4	Russia	1.5°×2.0°
MIROC5	Japan	1.4°×1.4°
MIROC-ESM	Japan	2.8°×2.8°
MIROC-ESM-CHEM	Japan	2.8°×2.8°
MPI-ESM-LR	Germany	1.9°×1.9°
MRI-CGCM3	Japan	1.1°×1.1°
NorESM1-M	Norway	1.9°×2.5°

The simulated results exhibit more or less differences between models even when the models forced by identical external forcing (e.g. green house gases), due to the differences in dynamical framework, parameterization schemes, and spatiotemporal resolutions. Moreover, it is hard to distinguish the merits or defects between models and to determine which models can estimate future climate change more accurately. Therefore, the MME method with equivalent weights, which is a commonly used method in projecting climate change, is applied in this study. Previous researches have suggested that the results of MME are more reliable compared to those of single model [19,20].

Because the horizontal resolution is different from model to model, in order to analyze MME results, all the model data grids are converted to 2.5°×2.5° latitude-longitude grid, which is the same with the grid for the reanalysis dataset used for evaluation. The reanalysis datasets used in this study are the National Centers for Environmental Prediction/National Center for Atmospheric Research (NCEP/NCAR) reanalysis data and the Global Precipitation Climatology Project (GPCP) precipitation data.

Interannual standard deviation (SD) and correlation coefficient are used to depict the intensity of interannual variability and the relationship between two variables, respectively. For observations, 48 years (1958–2005) of NCEP/NCAR reanalysis data and 29 years (1979–2007) of GPCP data are used. For models, about 100 years (1900–2005 for the 20th century and 2006–2099 for the 21st century) simulated outputs are used. The lengths of these time periods are adequate for reliably depicting intensity of both interannual

variability and relationship. The component of timescale greater than 9 years is filtered out before calculating the interannual SD and correlation coefficient.

2 A brief evaluation of the models' simulations

Figure 1 shows the climatology and SD of zonal wind at 200 hPa in summer (June to August). Climatologically, in the reanalysis data, the core of the EAJ is located at about 40°N, and the largest wind speed exceeds 30 m/s and is located in the northern Tibetan Plateau (Figure 1(a)). Although there are significant model-to-model differences, for instance, the maximum of zonal wind appears over North Pacific in some models (not shown), the MME simulation can reproduce well the spatial distribution of EAJ (Figure 1(b)). In the MME result, the core of the EAJ is located at 40°N and the maximum is in the northern Tibetan Plateau. The meander of the EAJ is also well captured. However, there are some differences between the MME and observation. First, the intensity of the EAJ in MME simulation is about 5 m/s weaker than the observed. Second, the width of EAJ in MME simulation is wider than the observed. These discrepancies are likely associated with the weaker meridional temperature gradient in models [8,21].

There are two maxima regions of interannual SD of 200-hPa zonal wind in the observation. One is resided in the mid-latitudes of East Asia, and extends eastward into the North Pacific, representing the considerable interannual variability of the EAJ [10]. The other area of great interannual SD is around the Ural Mountains (Figure 1(c)). The spatial distribution of the MME result is similar with the observation. The MME result can well reproduce the two maxima areas, although it fails to reproduce the detailed distribution in the mid-latitude of East Asia and the intensity of SD is weaker than the observed.

Figure 2 shows the climatology and interannual SD of precipitation in summer. There are four areas of rainfall maximum: the west coast of India, the eastern part of the Bay of Bengal, the east of South China Sea, and the Philippine Sea and extending east to the tropic Pacific (Figure 2(a)). The MME simulation captures well these features of the observed, although a stronger precipitation is over the south edge of the Tibetan Plateau (Figure 2(b)). In East Asia, the GPCP dataset shows a summer rain belt in a northeast-southwest direction, which includes South China, the Yangtze River Basin, the Korean Peninsula, and southern Japan. The MME reproduces roughly the northeast-southwest oriented rain belt, but this rain belt is southward shifted and weaker compared to the observation.

The spatial distribution of SD is similar with that of the climatological rainfall, i.e. the SD is larger over the region where the precipitation is larger, and vice versa (Figure 2(c)). This is well represented in the west coast of India, the eastern part of the Bay of Bengal and the east of South China Sea. However, the ratio of SD to total precipitation is relatively higher in the Philippine Sea, the western North Pacific and the East Asian summer rain belt. The MME simulation captures well the spatial distribution of SD, although it overestimates SD in the India Ocean and underestimates SD in the western North Pacific. Overall, interannual SD is reproduced better than climatological precipitation. The pattern correlation coefficient of SD (0.847) is slightly higher than that of climatological precipitation (0.829), suggesting that climate models have a stronger ability to reproduce SD than to reproduce climatological precipitation.

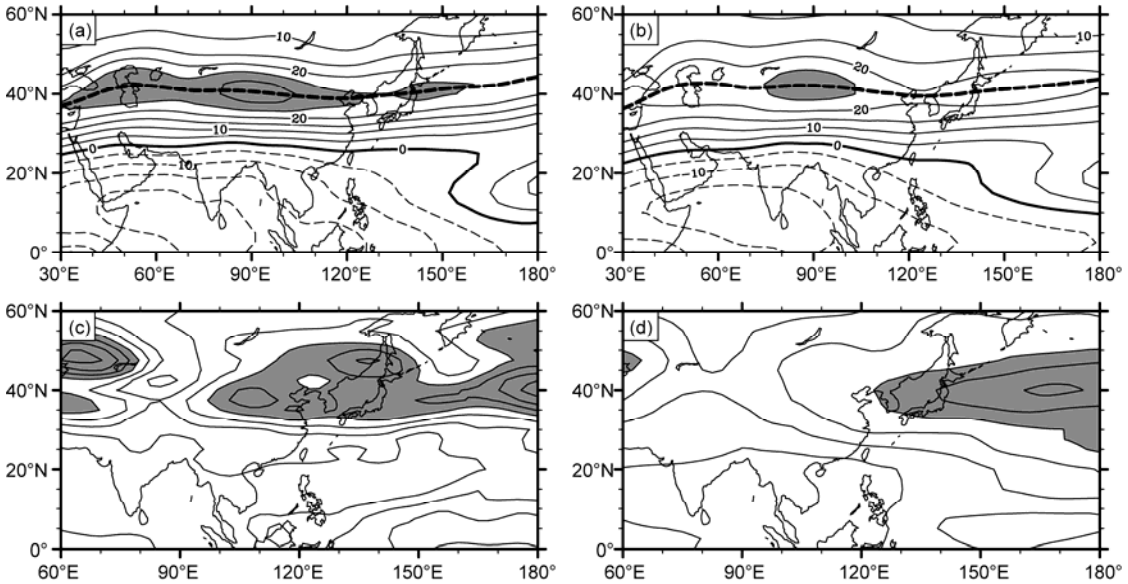

Figure 1 Climatology (a), (b) and SD (c), (d) of 200-hPa zonal wind in summer. (a), (c) For the observation; (b), (d) for the MME results. Contours interval is 5 m/s in (a) and (b), and is 0.5 m/s in (c) and (d). Zonal wind >25 m/s is shaded in (a) and (b), and SD >3.5 m/s is shaded in (c) and (d).

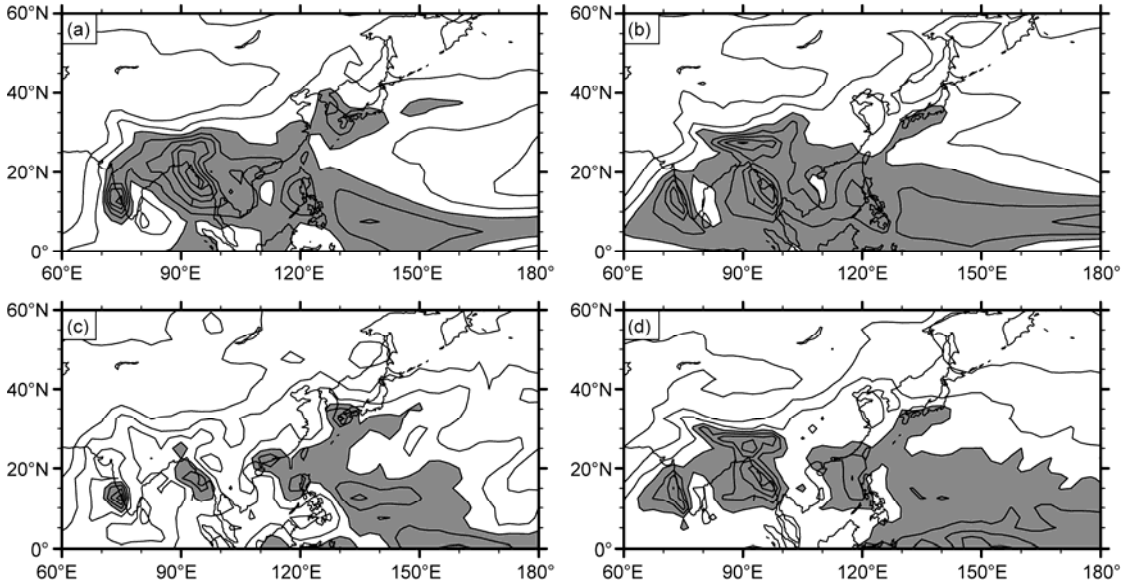

Figure 2 As in Figure 1, but for precipitation. Contours interval is 2 mm/d in (a) and (b), and is 0.4 mm/d in (c) and (d). Precipitation >6 mm/d is shaded in (a) and (b), and SD >1.6 mm/d is shaded in (c) and (d).

3 Projected future changes of EAJ, EASR and the relationship between them

Figure 3 shows projected changes of zonal wind at 200 hPa and precipitation under the scenario RCP4.5 in the year 2006–2099 compared to the 20th century. In the 21st century, zonal wind is increased more than 1 m/s along the 40°N over the central Asia (Figure 3(a)). This is consistent with the result of Zhang and Guo [15]. In the coastal area of East Asia and the western North Pacific, on which we focus, the zonal wind is slightly reduced. Summer precipitation is projected to be enhanced in the future in the domain of Figure 3(b) except some small and scattered areas. Precipitation in East Asia and surrounding areas also shows an increasing trend, especially in the western North Pacific and the Northeast Asia, which is roughly consistent with previous studies [2,4,22–24].

We also analyzed projected changes in zonal wind at 200 hPa and precipitation under the scenario RCP8.5 (not shown). The results are similar to those under the scenario RCP4.5, i.e. the 200-hPa zonal wind is not obviously changed while precipitation is increased in the coastal area of East Asia and the western North Pacific.

Figure 4 shows projected SD changes in zonal wind at 200 hPa and precipitation under the scenario RCP4.5. The SD of 200-hPa zonal wind is enhanced over East Asia and the western North Pacific in the 21st century (Figure 4(a)). Interestingly, the interannual SD shows a very weak change along 40°N, where the axis of the climatological EAJ is located, but increases both north and south to the axis. Therefore, it suggests that the meridional displacement, rather than the intensity, of the EAJ is expected to exhibit enhanced interannual variability under the global warming scenarios.

In the context of global warming, the interannual variability of precipitation is intensified over majority of regions, including East Asia and the western North Pacific (Figure 4(b)). The intensification is remarkable over South China and the subtropical western North Pacific. This is consistent with previous studies, which indicate that the interannual variability of summer precipitation over East Asia will be increased in the future [6,7].

The EAJ is closely related to East Asian summer precipitation. A southward (northward) displaced EAJ favors above-normal (below-normal) rainfall in East Asia. Next, we investigate the projected change in the relationship between East Asian summer precipitation and EAJ meridional displacement under the global warming.

In order to facilitate quantitative analysis of precipitation and EAJ, two indexes are used to characterize the East Asian precipitation and the meridional displacement of EAJ. First, we define an EAJ index (EAJI) by the difference between the 200 hPa zonal winds averaged over (120°–150°E, 30°–40°N) and (120°–150°E, 40°–50°N), following Lu [11]. A positive (negative) EAJI indicates a southward (northward) displacement of the EAJ. Second, an East Asian Summer Rainfall Index (EASRI) is defined by the summer mean precipitation averaged over the parallelogram region determined by the points (25°N, 100°E), (35°N, 100°E), (30°N, 160°E), and (40°N, 160°E), following Lu and Fu [7]. This region is used to mimic the East Asian subtropical rain belt in summer which has a slight southwest-northeast tilt. The correlation coefficient (CC) is used to represent the relationship between the two indexes.

Figure 5 shows the projected change in the interannual variability of EASRI under the scenarios RCP4.5 and

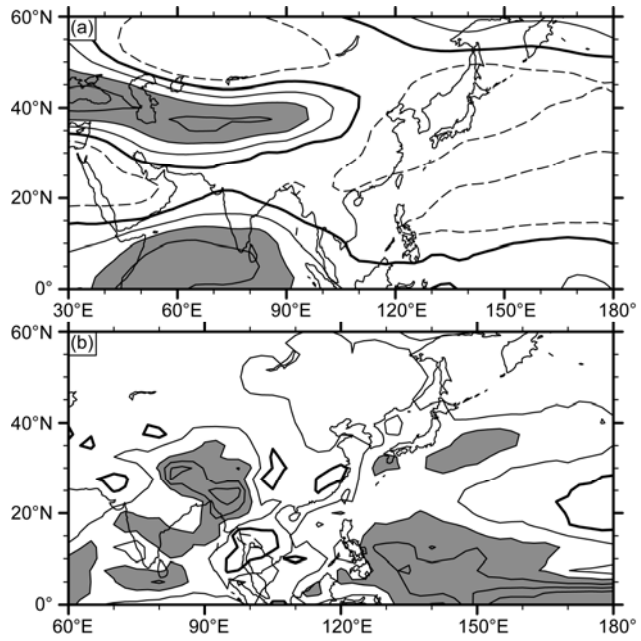

Figure 3 Projected changes in 200-hPa zonal wind (a) and precipitation (b) in the 21st century under the scenario RCP4.5. Contours interval is 0.5 m/s in (a) and 0.2 mm/d in (b). The shaded areas are for values greater than 1 m/s in (a) and 0.4 mm/d in (b).

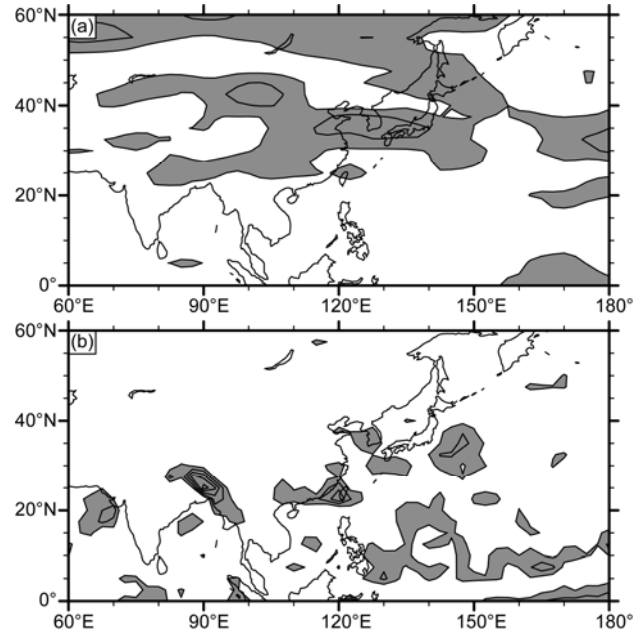

Figure 4 As in Figure 3, but for the SD. Contours interval is 0.1 m/s in (a) and 0.1 mm/d in (b). The shaded areas are for values greater than 0.1 m/s in (a) and greater than 0.1 mm/d in (b).

RCP8.5. The interannual variability in EASRI is intensified under the global warming scenarios. Almost all models suggest that the interannual variability in EASRI is enhanced under the scenario RCP4.5, except for the models CanESM2 and GISS-E2-R, which project slight weakened SD (<0.1). Similarly, except for the model Fgoals-g2, all models project enhanced interannual variability of EASR

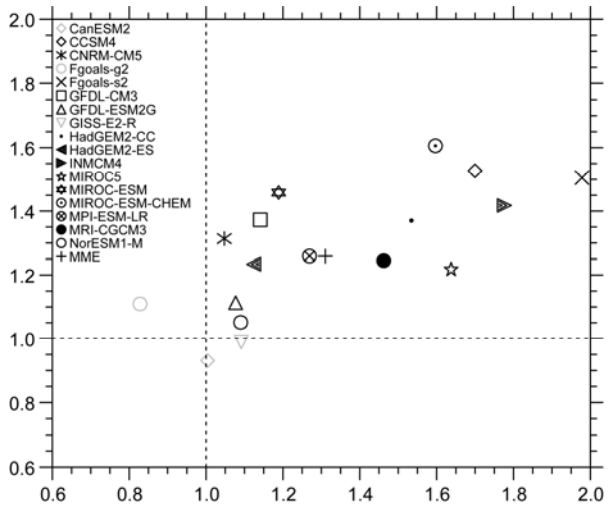

Figure 5 Projected change in the SD of EASRI under the scenarios RCP4.5 and RCP8.5. The abscissa is for the ratio of the SD between the scenario RCP8.5 and 20 C, and the ordinate is for the ratio between the scenario RCP4.5 and 20 C.

under the scenario RCP8.5. Ten models project a more remarkably enhanced interannual variability under the scenario RCP8.5 than under the scenario RCP4.5, implying that the greater green house gases emission, the greater interannual variability of EASR will experience.

Figure 6 shows the projected change in the relationship between the EAJ and EASR under the scenarios RCP4.5 and RCP8.5 in the 21st century. Under the scenario RCP4.5, most models (12 of 17) shows that the correlation coefficient is increased in the 21st century, i.e. the relationship of summer precipitation and the upper-tropospheric westerly jet over East Asia might be more closely in the 21st century. On the other hand, under the scenario RCP8.5, the correlation coefficient is increased in about half of models but decreased in another half, suggesting a great uncertainty in the change in relationship between EASR and EAJ under the scenario RCP8.5.

In the context of global warming, the intensified interannual variability of precipitation in East Asia may be one of the reasons for the stronger relationship between the EAJ and EASR. Since a precipitation anomaly in East Asia can cause the meridional displacement of EAJ [25], an enhanced interannual variability of East Asian rainfall may result in an intensified relationship between the EAJ and EASR. However, due to remarkable interdecadal variability in EAJ [26,27], the complicated mechanisms for the meridional displacement of EAJ, such as the feedback of transient eddy [28], and the existence of many factors, besides the EAJ, affecting the East Asian summer precipitation. Greater efforts are still necessary for illustrating possible change in the relationship between the EAJ and EASR. In particular, some studies suggested that the land surface temperature changes over Eurasia, which is related to the global warming, may also affect the EASR [29,30].

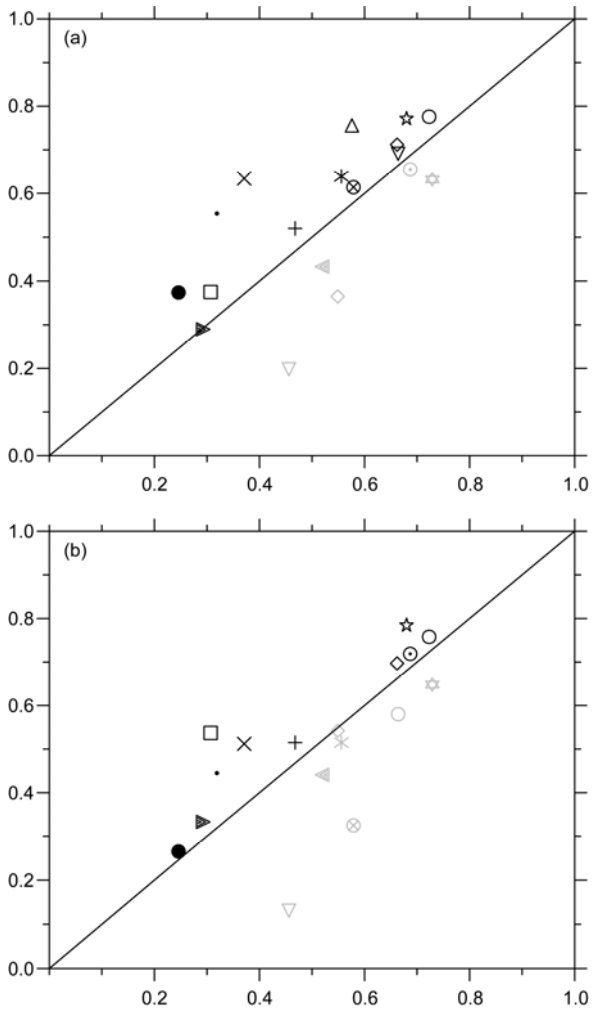

Figure 6 Projected change in the CC in the 21st century under the scenarios RCP4.5 and RCP8.5. The abscissa is the CC in 20 C, and the ordinate is the CC under the scenarios RCP4.5 and RCP8.5 in (a) and (b), respectively.

4 Conclusions

In this study, we investigated the projected changes in interannual variability of EAJ and EASR in the 21st century under scenarios RCP4.5 and RCP8.5, by analyzing the simulation of 17 CMIP5 models. The possible change in the relationship between the EASR and EAJ in the 21st century was also examined. Main results are summarized as follows.

(1) The simulation of MME can well reproduce the relatively stronger interannual variability in precipitation and EAJ over East Asia and the western North Pacific.

(2) The interannual variability in precipitation over East Asia and EAJ will be intensified in the 21st century under the scenarios RCP4.5 and RCP8.5.

(3) The relationship between the EASR and EAJ becomes closer in the 21st century in the context of global warming. However, great uncertainty is existed under the scenario RCP8.5, and the reasons for this uncertainty are unknown.

We thank two anonymous reviewers and Dr. Zhongda Lin for helpful comments and suggestions. We acknowledge the modeling groups, World Climate Research Programme's (*WCRP*) *Working Group on Coupled Modelling* (*WGCM*) *and the Program for Climate Model Diagnosis and Intercomparison* (*PCMDI*), *which is responsible for CMIP5. Support of this dataset is provided by the Office of Science, U.S. Department of Energy. This work was supported by the National Basic Research Program of China* (*2009CB421400*).

1 Bueh C, Cubasch U, Lin Y, et al. The change of North China climate in transient simulations using the IPCC SRES A2 and B2 scenarios with a coupled atmosphere-ocean general circulation model. Adv Atmos Sci, 2003, 20: 755–766
2 Kimoto M. Simulated change of the East Asian circulation under the global warming. Geophys Res Lett, 2005, 32: L16701
3 Kitoh A, Hosaka M, Adachi Y, et al. Future projections of precipitation characteristics in East Asia simulated by the MRI CGCM2. Adv Atmos Sci, 2005, 22: 467–478
4 Lee E J, Kwon W T, Baek H J. Summer precipitation changes in Northeast Asia from the AOGCM global warming experiments. J Meteor Soc Jpn, 2008, 86: 475–490
5 Wang H J, Sun J Q, Chen H P, et al. Extreme climate in China: Facts, simulation and projection. Meteorol Zeitschrift, 2012, 21: 279–304
6 Kripalani R H, Oh J H, Chaudhari H S. Response of the East Asian summer monsoon to doubled atmospheric CO_2: Coupled climate model simulations and projections under IPCC AR4. Theor Appl Clim, 2007, 87: 1–28
7 Lu R Y, Fu Y H. Intensification of East Asian summer rainfall interannual variability in the 21st century simulated by 12 CMIP3 coupled models. J Clim, 2010, 23: 3316–3331
8 Zhang Y C, Kuang X Y, Guo W D, et al. Seasonal evolution of the upper-tropospheric westerly jet core over East Asia. Geophys Res Lett, 2006, 33: L11708
9 Lin Z D, Lu R Y. Abrupt northward jump of the East Asian upper-tropospheric jet stream in mid-summer. J Meteorol Soc Jpn, 2008, 84: 857–866
10 Li C Y, Wang Z T, Lin S Z, et al. The relationship between East Asian summer monsoon activity and northward jump of upper westerly jet location (in Chinese). Chin J Atmos Sci, 2004, 28: 641–658
11 Lu R Y. Associations among the components of the East Asian summer monsoon system in the meridional direction. J Meteorol Soc Jpn, 2004, 82: 155–165
12 Xuan S L, Zhang Q Y, Sun S Q. Anomalous midsummer rainfall in Yangtze River-Huaihe River valleys and its association with the East Asia westerly jet. Adv Atmos Sci, 2011, 28: 387–397
13 Lin Z D, Lu R Y. Interannual meridional displacement of the East Asian upper-tropospheric jet stream in summer. Adv Atmos Sci, 2005, 22: 199–211
14 Liang X Z, Wang W C. Association between China monsoon rainfall and tropospheric jets. Q J Meteorol Soc, 1998, 124: 2597–2623
15 Zhang Y C, Guo L L. Multi-model ensemble simulated changes in the subtropical westerly jet over East Asia under the global warming condition (in Chinese). Sci Meteorol Sin, 2010, 30: 694–700
16 Sperber K, Potter G, Boyle J, et al. Simulation of the northern summer monsoon in the ECMWF model: Sensitivity to horizontal resolution. Mon Weather Rev, 1994, 122: 2461–2481
17 Gao X J, Xu Y, Zhao Z C, et al. Impacts of horizontal resolution and topography on the numerical simulation of East Asian precipitation (in Chinese). Chin J Atmos Sci, 2006, 30: 185–192
18 Kusunoki S, Yoshimura J, Yoshimura H, et al. Change of Baiu rain band in global warming projection by an atmospheric general circulation model with a 20-km grid size. J Meteorol Soc Jpn, 2006, 84: 581–611

19 Jiang D, Wang H J, Lang X. Evaluation of East Asian climatology as simulated by seven coupled models. Adv Atmos Sci, 2005, 22: 479–495
20 Xu C H, Shen X Y, Xu Y. An analysis of climate change in East Asia by using the IPCC AR4 simulations (in Chinese). Adv Clim Change Res, 2007, 3: 287–292
21 Cai Q Q, Zhou T J, Wu B, et al. The East Asian subtropical westerly jet and its interannual variability simulated by a climate system model FGOALS_gl (in Chinese). Acta Oceanol Sin, 2011, 33: 38–48
22 Bueh C. Simulation of the future change of East Asian monsoon climate using the IPCC SRES A2 and B2 scenarios. Chin Sci Bull, 2003, 48: 1024–1030
23 Shi Y, Gao X J, Wang Y G, et al. Simulation and projection of monsoon rainfall and rain patterns over eastern China under global warming by RegCM3. Atmos Oceanic Sci Lett, 2009, 2: 308–313
24 Bao Q. Projected changes in Asian summer monsoon in RCP scenarios of CMIP5. Atmos Oceanic Sci Lett, 2012, 5: 43–45
25 Lu R Y, Lin Z D. Role of subtropical precipitation anomalies in maintaining the summertime meridional teleconnection over the western North Pacific and East Asia. J Clim, 2009, 22: 2058–2072
26 Lu R Y, Ye H, Jhun J G. Weakening of interannual variability in the summer East Asian upper-tropospheric westerly jet since the mid-1990s. Adv Atmos Sci, 2011, 28: 1246–1258
27 Zhang Y C, Huang D Q. Has the East Asian westerly jet experienced a poleward displacement in recent decades? Adv Atmos Sci, 2011, 28: 1259–1265
28 Xiang Y, Yang X Q. The effect of transient eddy on interannual meridional displacement of summer East Asian subtropical jet. Adv Atmos Sci, 2012, 29: 484–492
29 Xu K, He J H, Zhu C W. The interdecadal linkage of the summer precipitation in eastern China with the surface air temperature over Lake Baikal in the past 50 years (in Chinese). Acta Meterorol Sin, 2011, 69: 570–580
30 Zhu C, Wang B, Qian W, et al. Recent weakening of northern East Asian summer monsoon: A possible response to global warming. Geophys Res Lett, 2012, 39: L09701